AJNR

MR Imaging Presentation of Intracranial Disease Associated with Langerhans Cell Histiocytosis

Daniela Prayer, Nicole Grois, Helmut Prosch, Helmut Gadner and Anthony J. Barkovich

AJNR Am J Neuroradiol 2004, 25 (5) 880-891
http://www.ajnr.org/content/25/5/880

AJNR Am J Neuroradiol 25:880–891, May 2004

MR Imaging Presentation of Intracranial Disease Associated with Langerhans Cell Histiocytosis

Daniela Prayer, Nicole Grois, Helmut Prosch, Helmut Gadner, and Anthony J. Barkovich

BACKGROUND AND PURPOSE: **Intracranial manifestations of Langerhans cell histiocytosis (LCH) are underestimated in frequency and diversity. We categorized the spectrum of MR imaging changes in LCH.**

METHODS: **We retrospectively reviewed 474 MR images in 163 patients with LCH and 55 control subjects. Lesions were characterized by anatomic region and signal intensity. Brain atrophy was assessed.**

RESULTS: **We noted osseous lesions in the craniofacial or skull bones in 56% of patients, meningeal lesions in 29%, and choroid-plexus involvement in 6%. In the hypothalamic-pituitary region, infundibular thickening occurred in 50%; pronounced hypothalamic mass lesions in 10%; and infundibular atrophy in 29%. The pineal gland had a cystic appearance in 28%, and pineal-gland enlargement (>10 mm) was noted in 14%. Nonspecific paranasal-sinus or mastoid opacifications were seen in 55% of patients versus 20% of controls, and accentuated Virchow-Robin spaces occurred in 70% of patients versus 27% of controls ($P < .001$). Intra-axial, white-matter parenchymal changes resulted in a leukoencephalopathy-like pattern in 36%. Enhancing lesions in a vascular distribution were noted in 5%. Gray-matter changes suggestive of neurodegeneration were identified in the cerebellar dentate nucleus in 40% and in the supratentorial basal ganglia in 26%. All patients with neurodegenerative lesions had lesions in the extra-axial spaces. Cerebral atrophy was found in 8%.**

CONCLUSION: **In LCH, cranial and intracranial changes at MR imaging include 1) lesions of the craniofacial bone and skull base with or without soft-tissue extension; 2) intracranial, extra-axial changes (hypothalamic-pituitary region, meninges, circumventricular organs); 3) intracranial, intra-axial changes (white matter and gray matter); and 4) cerebral atrophy.**

Langerhans cell histiocytosis (LCH) is a rare disease with an incidence of 0.2–2.0 cases per 100,000 children under 15 years of age. The frequency in adults is yet unknown (1). LCH is regarded as a reactive clonal disease of the monocyte-macrophage system and may affect almost any organ (2). The lesions are dominated by Langerhans cells, which are bone marrow derived cells of the dendritic cell line with antigen presenting and processing properties. They are involved in a variety of immune responses and are found in the normal brain parenchyma and pituitary gland (2, 3). Despite increasing understanding of dendritic cell biology, the pathophysiology of LCH remains enigmatic.

The hypothalamic-pituitary manifestations of LCH with the clinical hallmark of diabetes insipidus are well known (4, 5). However, other diverse forms of LCH-associated CNS involvement have been reported, though only in anecdotal case reports and small series. These other findings include infiltrating mass lesions with or without associated bone lesions and obscure neurodegenerative changes associated with profound neurologic disabilities (6–11). Intracranial lesions have been observed during the course of disease in patients with a history of proved LCH and also as the first and presenting LCH manifestations, in which case they can cause considerable diagnostic problems (7, 12, 13). The wide array of CNS changes, as visualized at MR imaging, has not been sufficiently described. Still, no morphologic patterns characteristic of LCH have been identified to facilitate prompt diagnosis.

In 1994, our group published a classification of the CNS lesions observed on MR images of 23 patients

Received April 25, 2003; accepted after revision October 15.

From the Department of Neuroradiology, University Clinic of Radiodiagnostics (D.P.), and the Children's Cancer Research Institute (N.G., H.P., H.G.), Vienna, Austria, and the Department of Neuroradiology, University of San Francisco, CA (A.J.B.).

Address reprint requests to Daniela Prayer, MD, University Clinic of Radiodiagnostics, Department of Neuroradiology, Waehringerguertel 18–20, Vienna 1090, Austria.

TABLE 1: Scheme for the evaluation of cranial MR images in patients with LCH

Anatomic Structure	Changes
Craniofacial bones and skull base	Bone destruction, tumorous infiltration, intracranial extension
Paranasal sinuses	
Ethmoidal	Bone destruction
Maxillar	Opacification (fluid intense, tissue intense)
Sphenoidal	Enhancement
Intracranial and extra-axial	
Meninges	
Epidural	With or without bone destruction
Subdural	Infiltration, enhancement, symmetry
Circumventricular organs*	Enlargement, cystic formation, enhancement, symmetry
Hypothalamic-pituitary region	
Anterior pituitary	Size (empty sella, atrophy, normal, enlarged), symmetry, enhancement
Posterior pituitary	Size, T1WI hyperintensity present or absent
Infundibulum	Size (measured in at least 2 planes) normal, thickened >2.6 mm, cranial-caudal different, threadlike <1 mm
Hypothalamus	Mass lesions, enhancement
Intracranial and intra-axial, parenchymal	
WM	
Vascular pattern	Symmetry
VRSs on T2WI†	Enhancement, space-occupying effect, edema
Perivascular spaces	Visibility on T2WI
Brainstem, pons	Leukoencephalopathy-like pattern
Cerebellar WM enhancement	T2WI hyperintensity, T1WI isointensity or hypointensity, not space-occupying
GM	
Basal ganglia	T1WI hyperintensity or hypointensity
Cerebellar dentate nuclei	T2WI isointensity, hypointensity, or hyperintensity
Atrophy	Localized, diffuse

* Pineal gland, ependyma, choroid plexus.

† VRS indicates Virchow-Robin space.

with LCH to provide a working scheme for the evaluation of suspected CNS LCH (14). In the framework of the large, multicentric LCH trials, a registry of LCH patients with CNS changes was established. Over the past years, information about 163 patients with 474 MR imaging studies was collected. On the basis of this uniquely large series, we could assess the broad spectrum of intracranial findings in LCH and describe the characteristic morphologic patterns. The distinctness of these morphologic features leads to a hypothesis about the possible pathophysiologic background of CNS LCH. Our new classification of cranial and intracranial LCH, should 1) provide a guideline for the evaluation of cranial MR images in patients with known or suspected CNS LCH to aid prompt diagnosis and 2) contribute to a better understanding of the underlying disease mechanisms with a potential impact on new therapeutic approaches.

Methods

Patients

Since 1993, 474 brain MR images of 163 patients with LCH have been sent to the study center for central review. This group included 65 female patients and 98 male patients for a female-to-male ratio of 1:1.5. At the time of the first image, patients' ages ranged 0.4–47 years (median, 8.2 years). At the time of diagnosis, patients ranged from neonates to adults aged 40.4 years (median, 2.8 years). The interval between the diagnosis of LCH and the first brain MR study was 1.2 years (in cases with primary CNS manifestations) to 20.6 years (median, 1.8 years).

To prove the importance of our findings, we compared the MR findings of the patients with LCH with those of a control group of 55 age-matched patients without LCH.

MR Imaging

MR images were obtained at 63 institutions in 20 countries by using various techniques. We considered only those MR studies that included 1) images in at least two section planes, 2) T2-weighted images (T2WI) and T1-weighted images (T1WI), and 3) images with and those without contrast enhancement that allowed proper assessment of intracerebral changes.

Inappropriate section thickness or image quality in the hypothalamic pituitary region, pineal gland, and skull base was not an exclusion criterion as long as the gray matter and white matter could be sufficiently assessed. As a consequence, the frequency of findings in the respective regions was related to the number of available imaging studies on which the structures of interest could be evaluated adequately. The image evaluation was done according to the scheme shown in Table 1. Follow-up studies performed at variable intervals were available in 99 patients.

Control Study

To assess the importance of opacifications in the paranasal sinuses and/or mastoids and the visibility of the Virchow-Robin spaces (VRS), we compared the MR images from 65 patients with those of 55 age-matched control subjects without LCH (Table 2). The control subjects underwent MR examinations at the Department for Neuroradiology, University Clinic of Vienna, for diverse indications. Twenty-seven control subjects had malignant brain tumors and had received chemotherapy or irradiation before the MR study. In the other 28 subjects, MR was performed for the evaluation of epilepsy ($n = 9$), cerebral malformations ($n = 3$), inflammatory disease ($n = 3$), metabolic disorders ($n =$

TABLE 2: Results of the control study

Finding	Patients with CNS LCH			Control Subjects			*P* Value
	No Treatment	With Treatment	All	Oncology Controls	Diverse Controls	All	
Sinus/mastoid opacification	11/19 (58%)	25/46 (54%)	36/65 (55%)	7/27 (26%)	4/28 (14%)	11/55 (25%)	.004
Dilated VRS	9/11 (81%)	21/32 (66%)	30/43 (70%)	8/27 (30%)	7/28 (25%)	15/55 (27%)	.001

3), vascular disease ($n = 3$), or neuropsychiatric disorders ($n = 7$). We included only MR imaging examinations performed between May and September to consider the possible influence of season and associated common cold infections on MR findings in the sinuses. Only studies that sufficiently assessed the paranasal sinuses and mastoid air cells were considered.

The 55 control subjects and 65 patients with LCH were aged 3 months to 47 years; this range corresponded to the age range of the 163 patients in the overall study group. To consider the possible influence of chemotherapy and/or cranial irradiation before the MR examination, both patients and control subjects were assigned to untreated and treated groups.

Statistical Analysis

To compare the frequency of VRS and sinus changes in LCH patients with and those without CNS disease and those with and those without treatment and also in control subjects with and those without treatment, we used the Fisher exact test and the χ^2 test, when appropriate. Because we found an overall significant difference in sinus changes between these groups, we additionally compared the frequency of sinus changes in untreated LCH patients with those of untreated nontumor control subjects and compared treated LCH patients with the tumor control subjects. In addition, we found an overall significant difference was for VRS; therefore, we also compared the patients with CNS LCH with the overall control group (Table 2).

Results

Changes in the Craniofacial Bone, Skull Base, and Sinus

In 125 studies (56%) of 91 patients, osseous lesions were observed in the craniofacial bones or skull base on at least one MR imaging study (Table 3). In 33 studies, only a single osseous lesion was seen, and in 92, as many as seven simultaneous lesions were observed in the craniofacial bones or skull base. Contrast enhancement was seen in patients with additional epidural involvement. The most frequently involved bones were the temporal bone (54%), the orbit (37%), the vault (47%), and the extraorbital facial bones (30%).

The paranasal sinuses or mastoids were opacified in 36 (55%) of 65 patients (Fig 1), as opposed to 11 (20%) 55 control subjects (Table 2). These changes were both of solid or fluid signal intensity. The ethmoid sinuses were involved in 49% of the patients with LCH; the mastoids in 43%; the maxillary sinuses in 26%; and the sphenoid sinus in 8%. No biopsy of the sinus changes were done. Bone destruction of the paranasal sinus was seen in six LCH cases with mass lesions involving the sphenoid, and in three LCH cases with ethmoid involvement.

TABLE 3: Morphology of intracranial lesions in 163 patients with 474 MR imaging studies

Lesion	MR Imaging Studies	Patients
Craniofacial bones and/or skull base	125	91
Paranasal sinuses	196	88
Ethmoidal	90	64
Maxillar	53	40
Sphenoidal	19	13
Intracranial and extra-axial changes		
Epidural	44	27
Subdural	31	21
Choroid plexus	24	10
Pineal gland		
Enlarged >10 mm	48	23
Cystic	102	46
Solid	111	56
Hypothalamic-pituitary region		
Anterior pituitary, assessable	241	139
Empty sella	11	8
Small	75	39
Normal	134	73
Enlarged	21	14
Posterior pituitary, assessable	248	124
Bright spot present	46	26
Bright spot absent	239	98
Pituitary stalk, assessable	393	137
Normal	188	87
Thickened >3 mm	140	68
Cranial-caudal difference	59	32
Threadlike <1 mm	65	40
Hypothalamic mass lesions	40	17
Intracranial and intra-axial changes		
WM changes, vascular pattern		
Visible VRSs	112*	54†
Space-occupying lesions	26	8
Leukoencephalopathy-like pattern		
Periventricular	24	8
Brain stem, pons	74	44
Cerebellar WN	76	39
GM changes		
Basal ganglia	74	42
Cerebellar dentate nuclei	139	65

* 196 analyzed.

† 88 analyzed.

Intracranial/Extra-Axial Changes

Dura-Based Masses.—Dura-based masses were seen 48 patients (29%) and involved the subdural spaces in 21 and the epidural spaces in 27. These masses were isointense to hypointense to brain on T1WI with inconstant contrast enhancement; they appeared hypointense on T2WI (Fig 2A). In four patients, histopathologic examination of surgical specimens from such lesions revealed active LCH or

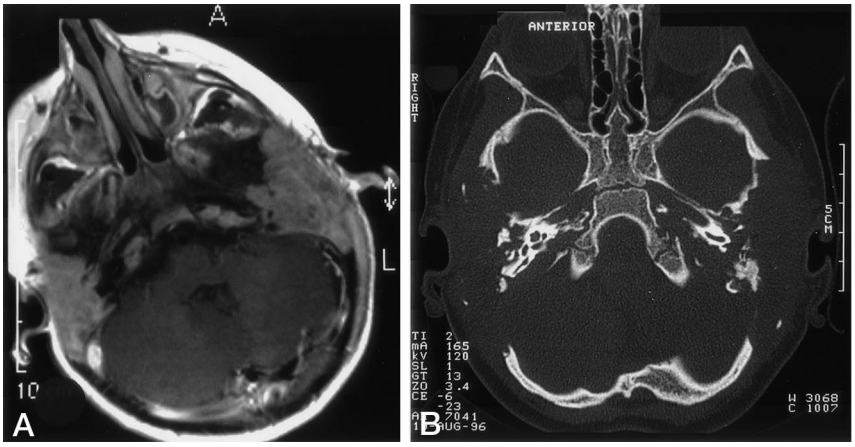

FIG 1. Mastoid involvement at the diagnosis of LCH in a 3-year-old patient.

A, Axial contrast-enhanced T1WI shows enhancing lesions in both mastoids.

B, Axial bone-window CT scan shows bilateral osseous destruction of the mastoids.

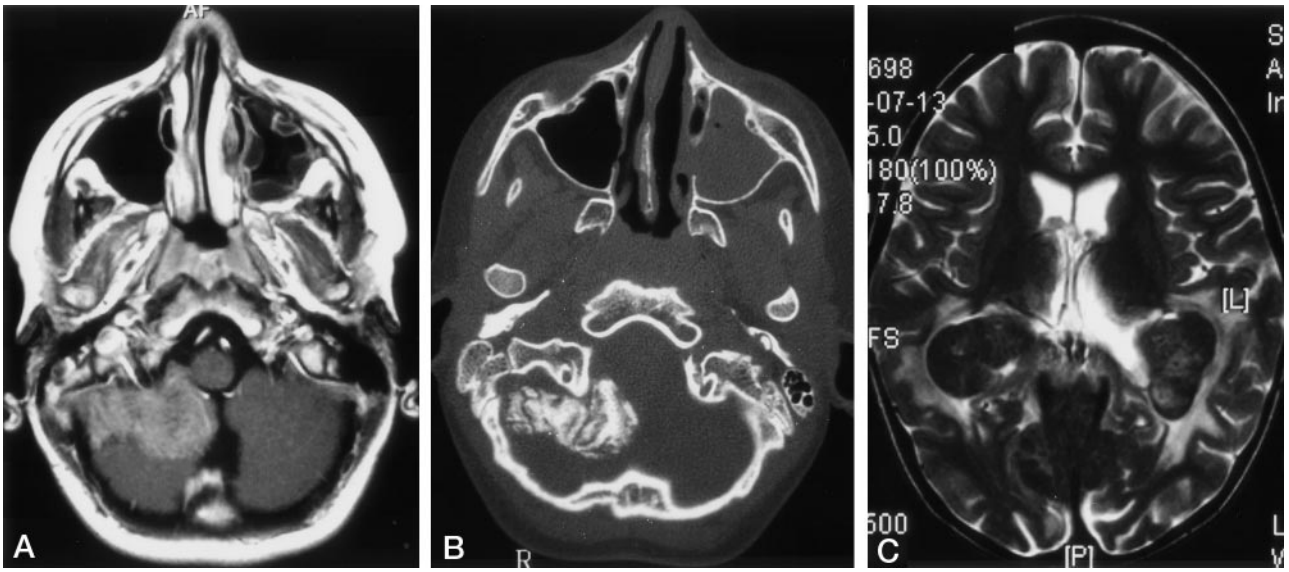

FIG 2. Images in two patients with LCH.

A and *B*, Lesions in a 13-year-old male patient at the diagnosis of LCH. Axial contrast-enhanced T1WI in *A* shows an extra-axial, enhancing, space-occupying lesion originating from the meninges. Axial bone-window CT scan in *B* shows calcification of the extra-axial lesion on the right side. Note the opacification of the left maxillary sinus.

C, Choriod plexus lesion in a 6-year-old girl with a 4.5-year history of LCH. Axial T2WIs show bilateral, hypointense masses in the choroid plexus and hyperintense changes in the parieto-occipital white matter.

fibroxanthomatous changes, consistent with "old burned out" LCH lesions. Two of 27 patients (four studies) had combined epidural and subdural involvement. Epidural involvement was combined with osseous lesions in all but one case. A lesion was assumed to lie in the epidural space when it could not or could hardly be delineated from the underlying bone (Fig 2A and B), or when the dura was displaced inward as a sign of a pathologic process between the skull and the dura as opposed to the normal position of the dura (adjacent to the skull) in cases of subdural lesions.

Choroid-Plexus Lesions.— Bilateral choroid-plexus lesions were found in 10 patients. All of these lesions had intermediate signal intensity on T1WI and marked hypointensity on T2WI (Fig 2B). These findings suggested calcification, which was proved in three cases with available CT scans. The appearance of the choroid plexus was interpreted as pathologic on the basis of the following criteria: size of more than one-third the width of the trigonum and/or plane, smooth calcifications that could not be mistaken for normal plexus calcifications (rare in children), a cloverleaf-like appearance that differed from the cauliflower-like appearance of the plexus papillomas, and/or increased size on follow-up studies. Other choroid-plexus lesions were not found. Enhancing thickening of the falx cerebri and tentorium were seen in one patient each. Infiltration of the falx and tentorium was diagnosed in cases of enhancing masses that led to thickening of these structures, as compared with other regions of the dura.

Pineal Gland.— The pineal gland had cystic changes in 46 patients (28%) and increased size (>10 mm) in 23 (14%), with a maximum size of 24 mm. Biopsy in one patient showed a xanthomatous granuloma.

Hypothalamic-Pituitary Involvement.— The thickness of the infundibulum was assessable in 393 studies in 137 patients. The infundibulum was normal (<3.00 mm in thickness) (15) on 188 MR studies in 87 pa-

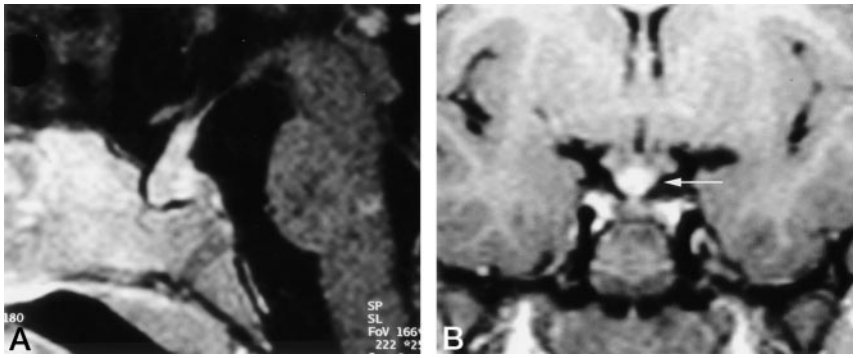

FIG 3. Images in two patients with LCH.
A, Thickened, enhancing pituitary stalk in a 2-year-old girl with a 1-year history of LCH and new-onset diabetes insipidus
B, Coronal contrast-enhanced T1WI in a 6-year-old girl obtained 2 years after the onset of diabetes insipidus. Image shows a thickened pituitary stalk at the cranial portion, in the region of the median eminence (*arrow*).

tients. Thickening of the infundibulum (>3.00 mm) was seen on 140 images in 68 patients (Fig 3A). In 17 cases, the diameter of the stalk could not be delineated because it was confluent with a hypothalamic mass. Histopathologic studies of biopsy samples from tumorous hypothalamic-pituitary lesions in six patients revealed active LCH. On 59 images (32 cases), the width of the infundibulum was different in its cranial and caudal portions (Fig 3B). Threadlike thinning of the stalk (<1 mm) was noted in 65 MR images (40 cases). Lack of infundibular contrast enhancement was seen on 36 images (24 cases), 12 of which depicted a threadlike infundibulum. Nineteen images revealed a normal-sized, nonenhancing infundibulum. In three cases (five images) the lack of contrast enhancement was seen with a thickened infundibulum; in two of these, the infundibulum was threadlike on the follow-up study. In six patients, histopathologic studies of tumorous hypothalamic-pituitary lesions revealed active LCH.

Intracranial/Intra-Axial Changes

Supratentorial White Matter.— Two major patterns of supratentorial white matter lesions were distinguished. The most frequent signal-intensity changes were prominent, dilated VRS, which was noted in 61% of patients with LCH (Fig 4A). In eight patients, images showed symmetrical lesions with prolonged T1 and T2 relaxation times following a vascular pattern, with strong contrast enhancement and mass effect (Fig 4B). Eight other patients had supratentorial white matter lesions with a leukoencephalopathy-like but no vascular pattern; that is, poorly defined patchy areas of low signal intensity on T1WI and high signal intensity on T2WI or proton density–weighted images without contrast enhancement (Fig 4C).

Infratentorial White Matter.— Infratentorial white matter lesions involved the pons in 44 patients (27%) (Fig 4D). These were associated with dentate nucleus changes in all but one. Pontine lesions consisted of T2WI hyperintensities, with either a microvascular pattern or patchiness. Enhancement was observed in eight cases (Fig 4E).

Deep Gray Matter.— Analysis of structures in the deep gray matter revealed a clear infratentorial predilection and symmetry of lesions in 65 patients (40%). Lesions in the dentate nucleus showed high signal intensity on T1WI; this was best depicted on T1WI with magnetization transfer contrast (Fig 5). In 44 of 65 patients, the dentate nucleus also appeared hyperintense with FLAIR and T2WI sequences (Fig 5). In this state, the formerly sharp margins of the region with abnormal signal intensity was blurred and faded into the surrounding white matter (Fig 5). As seen on follow-up images in a few patients, these changes occurred a few months to 6 years after the initial examination. The end stage of such changes consisted of sharply delineated CSF-intense holes, which included the dentate nucleus and the surrounding white matter (Fig 6) Space-occupying effect was not observed in pontine or dentate-nucleus lesions. In 35 patients, cerebellar changes occurred with or after pathologic signal-intensity changes in the basal ganglia on both sides. In 42 patients, the pallidum appeared hyperintense on T1WI and hypointense, isointense, or hyperintense on T2WIs (Fig 5); in three patients, the caudate nucleus was also involved. In four patients, the major supratentorial finding was a signal-intensity loss in the pallidum and putamen on T2WI. In these patients, this T2 signal-intensity loss was also seen in some structures of the midbrain (Fig 7).

All patients with parenchymal changes had lesions in the extra-axial spaces.

Brain Atrophy.— Signs of brain atrophy were seen in 13 patients. Five patients had localized atrophy of the cerebellum, which was combined with midbrain atrophy in four (Fig 7). One patient had localized midbrain atrophy.

Clinical Symptoms and Therapy

Patients with dilated VRS as the only parenchymal finding had no neurologic symptoms (Table 4). In 54 of 72 patients with parenchymal lesions (other than dilated VRS) at MR imaging, neurologic symptoms were reported. These ranged from subtle tremor and abnormal reflexes without disability in 13 patients to pronounced ataxia with severe impairment in 39. Eighteen patients with clear parenchymal changes in the cerebellum and/or basal ganglia were reported to be clinically asymptomatic. All 16 patients with leukoencephalopathy-like lesions or a pronounced vascular pattern had severe neurologic disabilities. All

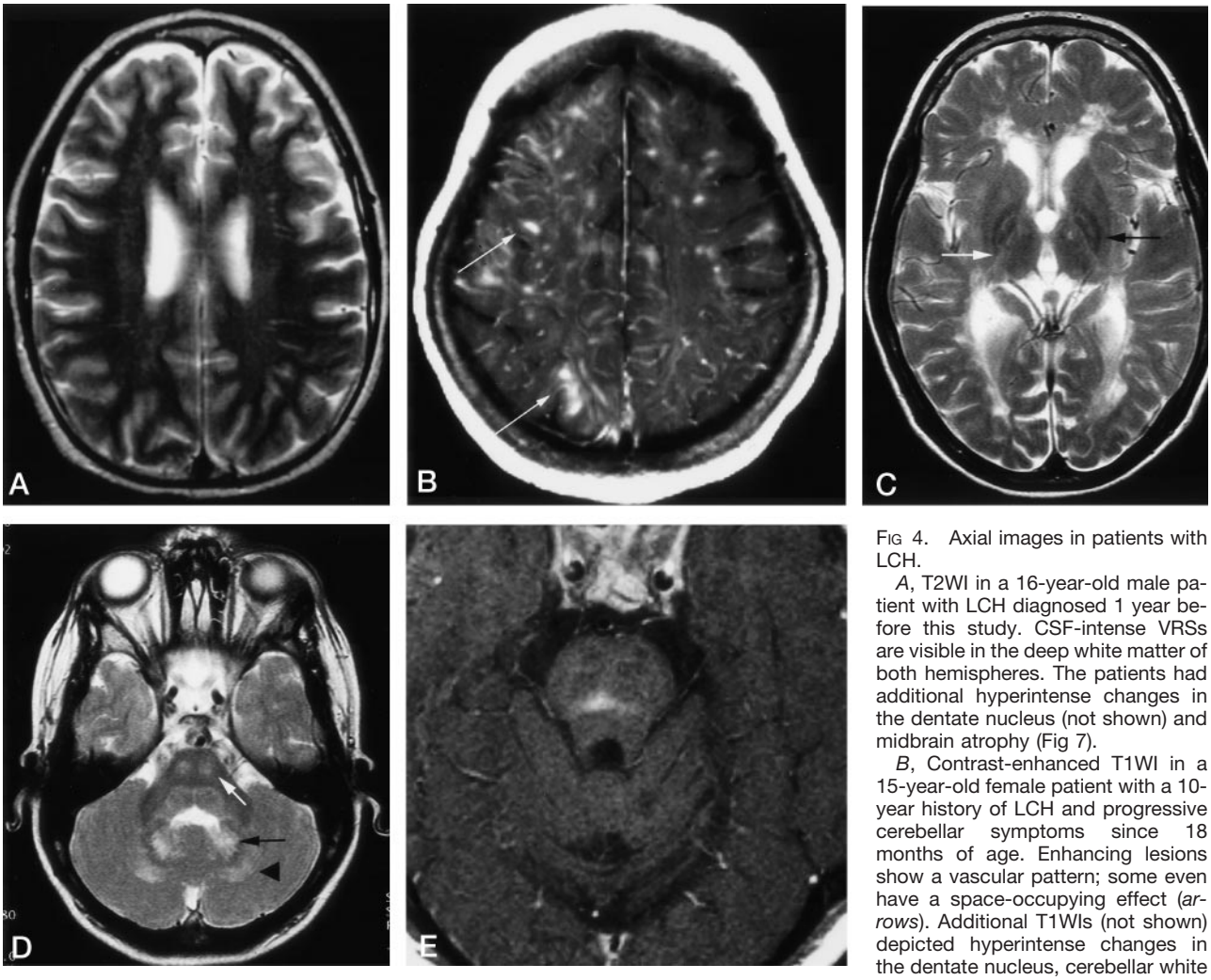

FIG 4. Axial images in patients with LCH.

A, T2WI in a 16-year-old male patient with LCH diagnosed 1 year before this study. CSF-intense VRSs are visible in the deep white matter of both hemispheres. The patients had additional hyperintense changes in the dentate nucleus (not shown) and midbrain atrophy (Fig 7).

B, Contrast-enhanced T1WI in a 15-year-old female patient with a 10-year history of LCH and progressive cerebellar symptoms since 18 months of age. Enhancing lesions show a vascular pattern; some even have a space-occupying effect (*arrows*). Additional T1WIs (not shown) depicted hyperintense changes in the dentate nucleus, cerebellar white matter, and basal ganglia.

C, T2WI in an 8-year-old patient with a 6-year history of LCH and severe neurologic disabilities. Hyperintense changes in the posterior limb of the internal capsule (*white arrow*) and periventricular region have a leukodystrophy-like pattern. Image also shows hypointensity of the pallidum with a hyperintense center (*black arrow*).

D, T2WI in the same patient as in *C* shows hyperintense changes in the central pons (*white arrow*), dentate nucleus (*black arrow*), and surrounding white matter (*arrowhead*).

E, Contrast-enhanced T1WI in a 28-year-old man with a 1-year history of LCH and moderate dysarthria and ataxia. Image shows an enhancing lesion in the center of the pons.

of these patients had additional neurodegenerative lesions in the cerebellum or basal ganglia.

Of the 72 patients with parenchymal changes, 62 had been treated with chemotherapy, and 15 received additional irradiation before CNS LCH was diagnosed. In contrast, 10 patients with lesions of the same MR appearance received neither cytostatic nor irradiation before the CNS lesions were diagnosed.

Six of the patients with parenchymal disease died from progressive neurologic deterioration. Three other patients with CNS LCH died: one from a hypothalamic syndrome, one from progressive LCH, and the third from a myelodysplastic syndrome.

Correlation with Histologic Findings

Biopsy results from the parenchymal lesions were available in 12 patients. In two patients, active LCH infiltrates with CD1a+ cells were proved by biopsy of space-occupying and contrast-enhancing lesions in the pons or cerebellum. In one patient (with a history of biopsy-proved extracranial LCH), a mass lesion (which was isointense to hyperintense on T1WI) involving the pons and cerebellum was shown to be an astrocytoma, grade III. Biopsy of cerebellar T2 prolongation in six patients revealed normal cerebellar tissue (in one patient) or loss of Purkinje cells with gliosis (in five patients). In two patients, superficial biopsy of supratentorial lesions yielded only fragments of normal gray and white matter.

Results of the Control Study

Paranasal Sinuses and Mastoid Opacification.—MR images in 65 LCH patients (46 treated, 19 untreated) and 55 control subjects (27 treated, 28 un-

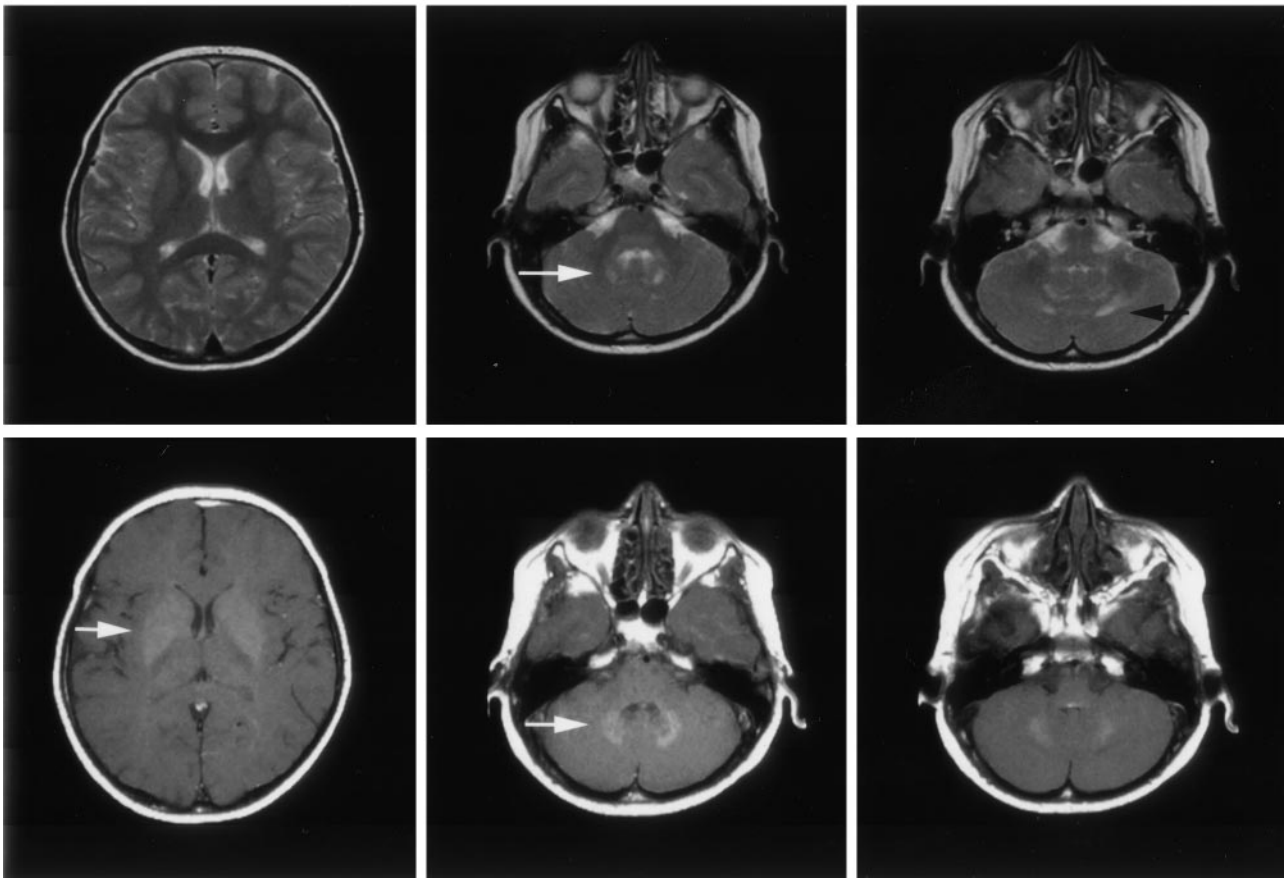

FIG 5. Axial images in a 9-year-old asymptomatic boy with a 7-year history of LCH. *Top row*, T2WI show the hyperintense appearance of the dentate nucleus (*white arrow*) and its surrounding white matter (*black arrow*). Note the normal appearance of the lentiform nucleus. *Bottom row*, T1WI with magnetization transfer contrast show the hyperintense appearance of the dentate nucleus and the lentiform nucleus (*white arrows*).

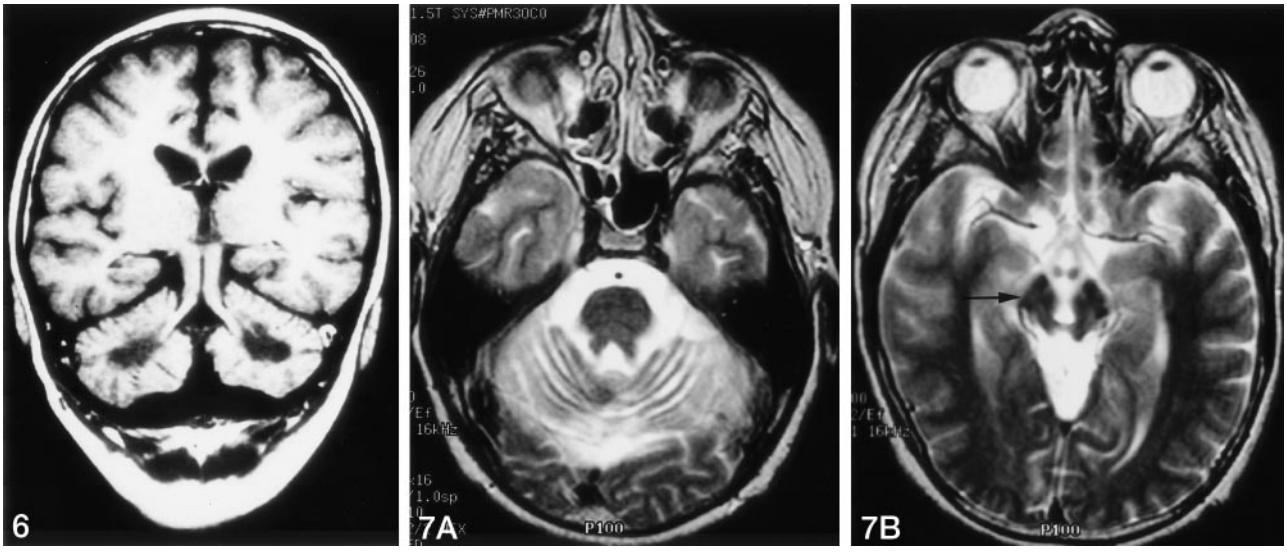

FIG 6. Coronal T1WI in a 12-year-old boy with a 10-year history of LCH, severe neurologic symptoms, and intellectual impairment. Image shows CSF-intense holes in the regions of the dentate nuclei.

FIG 7. Axial T2WIs in the same patient as in Figure 4A.

A, Cerebellar atrophy with thinned cerebellar peduncles.

B, Midbrain atrophy with wide interpeduncular cistern and distant mammillary bodies, with hypointensity of the pars compacta of the substantia nigra (*arrow*)

TABLE 4: Clinical information for 72 patients with intra-axial lesions

Information	Neurodegenerative (n = 72)	Leukoencephalopathy-like (n = 46)*	Vascular Pattern (n = 8)*
Age at diagnosis of LCH			
Mean	2 y 4 mo	2 y 8 mo	3 y 1 mo
Range	birth to 40 y	birth to 40 y	1 y 5 mo to 20 y
Age at diagnosis of CNS disease			
Mean	9 y	13 y 4 mo	13 y
Range	2 y 4 mo to 52 y	2 to 47 y	3 to 22 y
Chemotherapy before CNS disease			
No. of patients	62	32	6
Mean age	2 y 4 mo	2 y 8 mo	2 y
Age range	3 to 40 y	6 mo to 40 y	1 y 5 mo to 5 y 3 mo
Cranial radiotherapy before CNS disease			
No. of patients	15	9	1
Mean age	3 y 7 mo	5 y 6 mo	1 y 5 mo
Age range	1 y 5 mo to 27 y	2 y 7 mo to 28 y	Not applicable
Neurologic symptoms			
None	18	17	0
Subtle	15	6	0
Severe	39	23	8
Observation time			
Mean	8 y 3 mo	8 y 6 mo	10 y 7 mo
Range	1 mo to 20 y	1 mo to 20 y	3 to 17 y

* All patients had additional neurodegenerative lesions.

treated) were compared with respect to opacification in the paranasal sinuses and mastoids (Table 2). Configuration and signal intensity of these opacifying changes corresponded to fluid levels, polyps, and/or soft tissue. Contrast enhancement was seen in the last two conditions, which occurred in 36 (55%) LCH patients (25 treated, 11 untreated) and 11 (25%) control subjects (four untreated, seven treated). The χ^2 test showed a significant difference ($P < .005$). Comparison of the treated and untreated groups showed no significant difference.

Visible VRS.—T2WIs of 43 LCH patients (32 treated, 11 untreated) and 55 control subjects (27 treated, 28 untreated) were compared with respect to the visibility of the VRS. The VRS was visible in 30 (70%) of LCH patients (21 treated, nine untreated) and 15 (27%) control subjects (seven untreated, eight treated). The χ^2 test showed a significant difference ($P < .001$). Comparison of the treated and untreated groups showed no significant difference.

Discussion

In this comprehensive study, we described the impressively wide scope of brain changes in LCH, as shown on instantaneous MR images obtained at various times in the course of disease. Because of the retrospective and multicentric nature of the study, we could not provide standardized chronologic information about the evolution of various lesions on follow-up images. Also, we could not address the true incidence of CNS LCH. Earlier investigators estimated that the frequency of diabetes insipidus, the hallmark of hypothalamic pituitary region (HPR) involvement, is 5–50% (16), whereas the estimated incidence of neurodegenerative LCH is 1–3% (1, 16). Our recent observations in cases with only parenchymal abnormalities on MR images and no overt clinical signs or symptoms suggest that many cases are undiagnosed and that the actual incidence of CNS LCH might be higher than expected.

Cranial-facial involvement with osseous lesions in the bones of the orbits and the calvaria has long been recognized as a classic presentation of LCH (17–19). The observation of opacification in the paranasal sinuses or mastoids in 55% of LCH patients as opposed to 25% of controls was significant and striking. Because no histopathologic material was obtained in the patients of our series, the nature of the opacifications remains unclear. In most cases, possible LCH manifestations and other inflammatory or neoplastic processes cannot be distinguished. Opacifications of the paranasal sinuses and mastoid air cells are a common and nonspecific finding in the pediatric population and are seen with allergies and common colds (20, 21). We found that these changes were significantly less common in control subjects than in patients, taking into account the seasonal variations at the time of study. The predilection for these cavities (mastoid, ethmoidal sinus), which serve as conduits for cranial nerves, may result because the cranial nerves propagate immune processes from the cervical lymph nodes to intracerebral regions, where they primarily approach structures not protected by a blood-brain barrier (BBB) (22).

According to our series, the intracranial manifestations of LCH show a striking preference for regions without a BBB. Apart from the pituitary, extra-axial structures in the cranium include the meninges, the ependyma, the choroid plexuses, and the pineal gland. The pineal gland, together with median eminence, area postrema, organum vasculosum of the

lamina terminalis, subcommissural organ, and subfornical organ, form the circumventricular organs. None of these structures possess a BBB. This lack of BBB allows agents that normally do not have access to intracerebral regions to reach cerebral structures and trigger brain functions, and it allows other substances that cannot otherwise leave the brain (eg hypothalamic hormones) to reach their target organs (22). The hypothalamus itself is protected by the BBB; however, it forms a functional unit with the circumventricular organs. In addition, the neuroendocrine cell populations in the hypothalamus have been shown to project outside the BBB (22, 23). Therefore, these parts of the hypothalamic nuclei, which are functionally involved in the pathophysiology of CNS LCH, might reasonably be considered structures without a BBB.

The hypothalamic-pituitary axis is, by far, the most frequently involved intracranial region in LCH, and the resulting diabetes insipidus is a clinical hallmark of LCH. The imaging findings in central diabetes insipidus have been well described in the last decade. The most frequent morphologic change is a thickening (greater than 3 mm [15]) with enhancement of the pituitary stalk, accompanied by lack of the normal T1WI shortening in the posterior pituitary (24, 25). This so-called bright spot is related to the presence of vasopressin-containing granules (25–27). In addition, threadlike narrowing of the infundibulum with a maximum width less than 1 mm can be seen. The absence of hyperintensity in the posterior pituitary and the presence of an infundibular or hypothalamic mass are nonspecific findings. These can be seen in a variety of disorders, including intracranial tumors (mostly germinomas), granulomatous diseases (sarcoidosis, Wegener granulomatosis), leukemia, posttraumatic changes, autoimmune polyendocrinopathy, autoimmune infundibuloneurohypohysitis, brain malformations, familial disease, and idiopathic diabetes insipidus (15, 28–34).

Meningeal lesions usually have signal intensity corresponding to soft tissue (intermediate intensity on T1WI and T2WI with moderate or marked, uniform contrast-enhancement). Such lesions resemble lymphomatous, leukemic, or carcinomatous infiltrates. Choroid-plexus lesions, which might otherwise mimic plexus papillomas, are characterized by a marked signal intensity loss on T2WI, suggesting calcification. The presence of calcium was proved in two cases in which CT scans showed marked hyperattenuation.

The subfornical organ is adherent to the ventral surface of the fornix and protrudes into the third ventricle at the level of the interventricular foramina, partially covered by the choroid plexus. Involvement of this area might be suspected with lesions involving the choroid plexus and/or the ependyma of these regions.

The pineal gland, like the HPR, meninges, and choroid-plexus organs, does not possess a BBB (22). Therefore, it enhances after the administration of contrast material. The diagnosis of a pineal-gland lesion is not always straightforward and mainly based on its size and configuration (35). The high frequency of pineal cysts and enlarged pineal glands in patients with LCH remains a nonspecific but striking observation; this may reflect direct pineal infiltration by LCH or hyperplasia of the gland. Biopsy of a pineal-gland tumor in one patient revealed LCH infiltration and indicated that an association between HPR and pineal gland involvement in LCH, as observed in germinoma (36). However, in the absence of a histologic proof in the other patients, whether the morphologic appearance (size, solid vs cystic) of the pineal gland is related to the disease is unclear.

Intra-axial brain parenchymal changes showed different patterns. The second most frequent presentation of CNS LCH, apart from extra-axial HPR disease, was involvement of the cerebellum, basal ganglia, and pons. Clinically, this pattern of involvement was associated with a neurodegenerative syndrome of highly variable severity and course. The symptoms ranged from subtle tremor to profound disabilities, including ataxia, dysarthria, and psychomotor deterioration. Some patients with follow-up studies initially presented with slight hyperintensity of the dentate nucleus on T1WI; this appearance was followed by development hypointensity or hyperintensity on T2WI, with subsequent extension of T2 hyperintensity to the perinuclear white matter over months or years. Some patients with significant neurologic impairment ultimately developed CSF-intensity holes in the cerebellum. In 13 patients, T1WI hyperintensity limited to the dentate nucleus persisted for years without neurologic deterioration. From the few cases that we were able to follow up, neurologic impairment seemed to become clinically apparent when the signal-intensity abnormality extended into the cerebellar white matter.

These infratentorial changes were frequently associated with T1WI hyperintensity of the basal ganglia. Others have also reported this pathologic MR appearance of the basal ganglia and cerebellum (9, 37). The pathologic signal intensity in the basal ganglia and dentate nucleus of the cerebellum resemble the pattern of multiple-system degeneration. However, the term multiple-system atrophy, as defined by Gilman et al (38), does not seem to be entirely adequate in the neurodegenerative form of LCH. Multiple-system atrophy is a sporadic progressive neurodegenerative disorder with Parkinson-like, pyramidal, cerebellar, autonomic or bladder dysfunction, with involvement of the nigrostriatal system. Even if some these clinical criteria are fulfilled, overt autonomic dysfunction has not been reported in LCH CNS; in addition, the onset of complaints before the 3rd decade of life has been defined as an exclusion criterion for multiple-system atrophy (38, 39). The neuropathologic changes in multiple-system atrophy consist of cytoplasmic glial inclusions with neuronal cell loss, reactive astrogliosis, and microgliosis (40, 41). The few available biopsy specimens in CNS LCH, derived from mainly the cerebellum have shown loss of Purkinje cells with gliosis. Cytoplasmic inclusions have not been reported so far.

The white matter changes that we observed consisted of two patterns: a vascular pattern and a leukoencephalopathy pattern. In the vascular pattern, enlarged VRSs were identified in the deep white matter of the hemispheres on T2WIs. They ranged from barely visible (corresponding to a width of about 2 mm) to markedly enlarged and contrast enhancing, following the distribution of the perivascular spaces. Because enlarged VRSs are not necessarily pathologic and because they are seen with many other conditions (42–47), T2WIs were evaluated in an age-matched control group of children without LCH or vascular or seizure disorders. Interestingly, accentuated VRSs on T2WIs were considerably more common in LCH patients than in control subjects.

This vascular pattern was found incidentally in neurologically asymptomatic patients, in severely impaired patients, and in patients with and those without other CNS findings. Perivascular spaces that surround the penetrating arteries have been recognized as the lymphatic clefts of the CNS (48). Thus, they are involved in CNS immune responses to viral infection and autoimmune diseases (49, 50). Widening of these spaces leads to the imaging pattern of pronounced VRSs. In patients with LCH, pronounced VRSs may indicate an underlying cerebral immune process. They may also be secondary to cerebral atrophy, but severe atrophy was seen in only a few patients and always localized to infratentorial regions. The enhancement observed in eight patients might be attributed to breakdown of the BBB, which was possibly caused by LCH infiltration or a collapse of the immune defense mechanisms in the VRSs.

The leukoencephalopathy pattern was seen in severely disabled patients only. Imaging showed diffuse or patchy, usually symmetrical, involvement of the white matter without a clear vascular distribution. In most cases, supratentorial lesions were confluent and predominantly periventricular, with blurred margins. Breakdown of the BBB was present in a few severely disabled patients. In two patients, T2WIs showed a leukoencephalopathy-like pattern, while enhancing vascular structures were seen on T1WIs. Thus, the two described imaging patterns may possibly correspond to different manifestations of the same process. Regarding the leukoencephalopathy-like pattern, the differential diagnoses includes acute disseminated encephalomyelitis, acute multiphasic disseminated encephalitis, and disseminated encephalitis (51). Other differential diagnoses include diverse metabolic or degenerative disorders (52) and leukoencephalopathy secondary to chemotherapy and/or radiation therapy (53–55). Interestingly, 10 patients in our series had not received therapy before such white matter changes were diagnosed; therefore, these lesions seem to have been related to LCH rather than treatment. Associated changes in the infratentorial white matter may have been due to Wallerian degeneration primarily, as they were predominantly associated with degenerative lesions of the dentate nucleus.

Changes similar to those seen in the dentate nucleus are known to occur in a variety of neurodegenerative diseases. The dentate nucleus seems to be a cardinal target in corticobasal degeneration (56), hereditary dentatorubral-pallidoluysian atrophy, Machado-Joseph disease (57), and progressive supranuclear palsy (58). In children, T2 prolongation in the dentate nucleus may also indicate infantile neuroaxonal dystrophy or Krabbe disease, whereas T2 shortening in the pallida suggests Hallervorden-Spatz syndrome (59, 60). Additionally, degeneration of the dentate nucleus may be an inconstant part of different hereditary ataxias; when present, it is associated with poor prognosis (61). Degenerative changes of the cerebellum are also known to develop in paraneoplastic syndromes (62, 63). However, antineuronal antibodies, which were identified in other paraneoplastic syndromes (64), have not been detected in LCH so far (6). Furthermore, cerebellar degeneration and atrophy are typical features of metabolic diseases such as mitochondrial abnormalities in the dentate nucleus in conjunction with loss of Purkinje cells and spongiform degeneration of the cerebellar white matter, as seen in Kearns-Sayre syndrome (65) and myoclonus epilepsy with ragged red fibers (66). MR changes of the basal ganglia and the dentate nucleus are also the morphologic hallmark in cerebrotendinous xanthomatosis (67).

We found that involvement of the brain stem (particularly the pons) with intraparenchymal LCH was associated with poor prognosis (68). About 88% of patients with brain stem involvement had severe neurologic impairment. All but two patients who died had brain stem lesions. All patients with a vascular or leukoencephalopathy-like pattern that extended to infratentorial regions experienced rapidly progressive neurologic deterioration.

Atrophy was not a common finding in our series. Global atrophy was diagnosed in only seven individuals (all with several follow-up studies). Although it was infrequent and may be regarded as of questionable clinical importance, it was in these patients with CNS LCH and therefore retained in the classification system. Localized atrophy that mirrors irreversible tissue loss most frequently involved the cerebellar hemispheres and was always associated with a symptomatic, progressive neurodegenerative syndrome.

Conclusions

The wide spectrum of intracranial findings in LCH patients can be classified into four major groups according to their anatomic topography and signal-intensity pattern. Group 1 includes osseous lesions in the craniofacial bones and/or skull base with or without soft-tissue extension. Group 2 is an intracranial and extra-axial disease in the hypothalamic-pituitary region; meninges; and other circumventricular organs, including the pineal gland, choroid plexus, and ependyma. Group 3 is intra-axial parenchymal disease in the gray matter or white matter, with a striking symmetry of the lesions and a clear predominance of a neurodegenerative pattern in the cerebellum and basal ganglia. Group 4 is localized or diffuse atrophy.

These cranial and intracranial manifestations of LCH-associated CNS disease occur in typical patterns or combinations that may be suggestive of LCH, even in the absence of a history of LCH or extracranial signs or symptoms of LCH. Isolated diabetes insipidus with morphologic changes in the HPR should always prompt a careful diagnostic search for other intracranial and extracranial LCH-specific lesions. Also, a neurodegenerative syndrome with lesions in the cerebellum and basal ganglia or poorly marginated and symmetrical white matter changes in the absence of typical signs or symptoms of leukoencephalopathy should lead to the differential diagnosis of LCH followed by an adequate diagnostic evaluation.

References

1. **A multicentre retrospective survey of Langerhans' cell histiocytosis: 348 cases observed between 1983 and 1993: The French Langerhans' Cell Histiocytosis Study Group.** *Arch Dis Child* 1996;75:17–24
2. Arceci RJ. **The histiocytoses: the fall of the Tower of Babel.** *Eur J Cancer* 1999;35:747–767
3. Egeler RM, D'Angio GJ. **Langerhans cell histiocytosis.** *J Pediatr* 1995;127:1–11
4. Grois N, Flucher-Wolfram B, Heitger A, Mostbeck GH, Hofmann J, Gadner H. **Diabetes insipidus in Langerhans cell histiocytosis: results from the DAL-HX 83 study.** *Med Pediatr Oncol* 1995;24:248–256
5. Nanduri VR, Bareille P, Pritchard J, Stanhope R. **Growth and endocrine disorders in multisystem Langerhans' cell histiocytosis.** *Clin Endocrinol (Oxf)* 2000;53:509–515
6. Grois N, Barkovich AJ, Rosenau W, Ablin AR. **Central nervous system disease associated with Langerhans' cell histiocytosis.** *Am J Pediatr Hematol Oncol* 1993;15:245–254
7. Bergmann M, Yuan Y, Bruck W, Palm KV, Rohkamm R. **Solitary Langerhans cell histiocytosis lesion of the parieto-occipital lobe: a case report and review of the literature.** *Clin Neurol Neurosurg* 1997;99:50–55
8. Cervera A, Madero L, Garcia Penas JJ, et al. **CNS sequelae in Langerhans cell histiocytosis: progressive spinocerebellar degeneration as a late manifestation of the disease.** *Pediatr Hematol Oncol* 1997;14:577–584
9. Saatci I, Baskan O, Haliloglu M, Aydingoz U. **Cerebellar and basal ganglion involvement in Langerhans cell histiocytosis.** *Neuroradiology* 1999;41:443–446
10. Hund E, Steiner H, Jansen O, Sieverts H, Sohl G, Essig M. **Treatment of cerebral Langerhans cell histiocytosis.** *J Neurol Sci* 1999;171:145–152
11. Barthez MA, Araujo E, Donadieu J. **Langerhans cell histiocytosis and the central nervous system in childhood: evolution and prognostic factors. Results of a collaborative study.** *J Child Neurol* 2000;15:150–156
12. Braier J, Chantada G, Rosso D, et al. **Langerhans cell histiocytosis: retrospective evaluation of 123 patients at a single institution.** *Pediatr Hematol Oncol* 1999;16:377–385
13. Kaltsas GA, Powles TB, Evanson J, et al. **Hypothalamo-pituitary abnormalities in adult patients with langerhans cell histiocytosis: clinical, endocrinological, and radiological features and response to treatment.** *J Clin Endocrinol Metab* 2000;85:1370–1376
14. Grois N, Tsunematsu Y, Barkovich AJ, Favara BE. **Central nervous system disease in Langerhans cell histiocytosis.** *Br J Cancer Suppl* 1994;23:S24–S28
15. Maghnie M, Cosi G, Genovese E, et al. **Central diabetes insipidus in children and young adults.** *N Engl J Med* 2000;343:998–1007
16. Grois NG, Favara BE, Mostbeck GH, Prayer D. **Central nervous system disease in Langerhans cell histiocytosis.** *Hematol Oncol Clin N Am* 1998;12:287–305
17. Hand A. **Defects of Membraneous Bones,** *Exophthalmus and Polyuria in Childhood: Is it Dyspituitarism? Am J Med Sci* 1921;162:509–515
18. Holbach LM, Colombo F, Heckmann JG, Strauss C, Dobig C. **[Langerhans-cell histiocytosis of the orbit; diagnosis, treatment and outcome in three patients—children and adults].** *Klin Monatsbl Augenheilkd* 2000;217:370–373
19. Char DH, Ablin A, Beckstead J. **Histiocytic disorders of the orbit.** *Ann Ophthalmol* 1984;16:867–863
20. Gordts F, Clement PA, Buisseret T. **Prevalence of paranasal sinus abnormalities on MRI in a non-ENT population.** *Acta Otorhinolaryngol Belg* 1996;50:167–170
21. Maly PV, Sundgren PC. **Changes in paranasal sinus abnormalities found incidentally on MRI.** *Neuroradiology* 1995;37:471–474
22. Ganong WF. **Circumventricular organs: definition and role in the regulation of endocrine and autonomic function.** *Clin Exp Pharmacol Physiol* 2000;27:422–427
23. Millington GW, Tung YC, Hewson AK, O'Rahilly S, Dickson SL. **Differential effects of alpha-, beta- and gamma(2)-melanocyte-stimulating hormones on hypothalamic neuronal activation and feeding in the fasted rat.** *Neuroscience* 2001;108:437–445
24. Maghnie M, Genovese E, Bernasconi S, Binda S, Arico M. **Persistent high MR signal of the posterior pituitary gland in central diabetes insipidus.** *AJNR Am J Neuroradiol* 1997;18:1749–1752
25. Holder CA, Elster AD. **Magnetization transfer imaging of the pituitary: further insights into the nature of the posterior 'bright spot&quot.** *J Comput Assist Tomogr* 1997;21:171–174
26. Kucharczyk J, Kucharczyk W, Berry I, et al. **Histochemical characterization and functional significance of the hyperintense signal on MR images of the posterior pituitary.** *AJR Am J Roentgenol* 1989;152:153–157
27. Kurokawa H, Fujisawa I, Nakano Y, et al. **Posterior lobe of the pituitary gland: correlation between signal intensity on T1-weighted MR images and vasopressin concentration.** *Radiology* 1998;207:79–83
28. Bullmann C, Faust M, Hoffmann A, et al. **Five cases with central diabetes insipidus and hypogonadism as first presentation of neurosarcoidosis.** *Eur J Endocrinol* 2000;142:365–372
29. Czernichow P, Garel C, Leger J. **Thickened pituitary stalk on magnetic resonance imaging in children with central diabetes insipidus.** *Horm Res* 2000;53(Suppl 3):61–64
30. Masera N, Grant DB, Stanhope R, Preece MA. **Diabetes insipidus with impaired osmotic regulation in septo-optic dysplasia and agenesis of the corpus callosum.** *Arch Dis Child* 1994;70:51–53
31. Frangoul HA, Shaw DW, Hawkins D, Park J. **Diabetes insipidus as a presenting symptom of acute myelogenous leukemia.** *J Pediatr Hematol Oncol* 2000;22:457–459
32. Katzman GL, Langford CA, Sneller MC, Koby M, Patronas NJ. **Pituitary involvement by Wegener's granulomatosis: a report of two cases.** *AJNR Am J Neuroradiol* 1999;20:519–523
33. Gagliardi PC, Bernasconi S, Repaske DR. **Autosomal dominant neurohypophyseal diabetes insipidus associated with a missense mutation encoding Gly23–>Val in neurophysin II.** *J Clin Endocrinol Metab* 1997;82:3643–3646
34. Maghnie M. **Lymphocytic hypophysitis and central diabetes insipidus during adolescence: what are the criteria for diagnosis?** *Eur J Pediatr* 1998;157:693–694
35. Sumida M, Barkovich AJ, Newton TH. **Development of the pineal gland: measurement with MR.** *AJNR Am J Neuroradiol* 1996;17:233–236
36. Sugiyama K, Uozumi T, Kiya K, et al. **Intracranial germ-cell tumor with synchronous lesions in the pineal and suprasellar regions: report of six cases and review of the literature.** *Surg Neurol* 1992;38:114–120
37. Brunberg JA. **Hyperintense basal ganglia on T1-weighted MR in a patient with Langerhans cell histiocytosis.** *AJNR Am J Neuroradiol* 1996;17:1193–1194
38. Gilman S, Low PA, Quinn N, et al. **Consensus statement on the diagnosis of multiple system atrophy.** *J Neurol Sci* 1999;163:94–98
39. Schrag A, Good CD, Miszkiel K, et al. **Differentiation of atypical parkinsonian syndromes with routine MRI.** *Neurology* 2000;54:697–702
40. Schwarz J, Weis S, Kraft E, et al. **Signal changes on MRI and increases in reactive microgliosis, astrogliosis, and iron in the putamen of two patients with multiple system atrophy.** *J Neurol Neurosurg Psychiatry* 1996;60:98–101
41. Wenning GK, Braune S. **Multiple system atrophy: pathophysiology and management.** *CNS Drugs* 2001;15:839–852
42. Schick S, Gahleitner A, Wober-Bingol C, et al. **Virchow-Robin spaces in childhood migraine.** *Neuroradiology* 1999;41:283–287
43. Artigas J, Poo P, Rovira A, Cardo E. **Macrocephaly and dilated Virchow-Robin spaces in childhood.** *Pediatr Radiol* 1999;29:188–190
44. Rollins NK, Deline C, Morriss MC. **Prevalence and clinical significance of dilated Virchow-Robin spaces in childhood.** *Radiology* 1993;189:53–57

45. Berkefeld J, Enzensberger W, Lanfermann H. **Cryptococcus meningoencephalitis in AIDS: parenchymal and meningeal forms.** *Neuroradiology* 1999;41:129–133
46. Kanpittaya J, Jitpimolmard S, Tiamkao S, Mairiang E. **MR findings of eosinophilic meningoencephalitis attributed to Angiostrongylus cantonensis.** *AJNR Am J Neuroradiol* 2000;21:1090–1094
47. Lynch SA, Hall K, Precious S, Wilkies AO, Hurst JA. **Two further cases of Sener syndrome: frontonasal dysplasia and dilated Virchow-Robin spaces.** *J Med Genet* 2000;37:466–470
48. Aloisi F, Ria F, Adorini L. **Regulation of T-cell responses by CNS antigen-presenting cells: different roles for microglia and astrocytes.** *Immunol Today* 2000;21:141–147
49. Weller RO. **Pathology of cerebrospinal fluid and interstitial fluid of the CNS: significance for Alzheimer disease, prion disorders and multiple sclerosis.** *J Neuropathol Exp Neurol* 1998;57:885–894
50. Weller RO, Engelhardt B, Phillips MJ. **Lymphocyte targeting of the central nervous system: a review of afferent and efferent CNS-immune pathways.** *Brain Pathol* 1996;6:275–288
51. Dale RC, de Sousa C, Chong WK, Cox TC, Harding B, Neville BG. **Acute disseminated encephalomyelitis, multiphasic disseminated encephalomyelitis and multiple sclerosis in children.** *Brain* 2000; 123(Pt 12):2407–2422
52. Kolodny EH. **Dysmyelinating and demyelinating conditions in infancy.** *Curr Opin Neurol Neurosurg* 1993;6:379–386
53. Lovblad K, Kelkar P, Ozdoba C, Ramelli G, Remonda L, Schroth G. **Pure methotrexate encephalopathy presenting with seizures: CT and MRI features.** *Pediatr Radiol* 1998;28:86–91
54. Rabin BM, Meyer JR, Berlin JW, Marymount MH, Palka PS, Russell EJ. **Radiation-induced changes in the central nervous system and head and neck.** *Radiographics* 1996;16:1055–1072
55. Hertzberg H, Huk WJ, Ueberall MA, et al. **CNS late effects after ALL therapy in childhood, I: Neuroradiological findings in long-term survivors of childhood ALL–an evaluation of the interferences between morphology and neuropsychological performance—The German Late Effects Working Group.** *Med Pediatr Oncol* 1997;28:387–400
56. Su M, Yoshida Y, Hirata Y, Satoh Y, Nagata K. **Degeneration of the cerebellar dentate nucleus in corticobasal degeneration: neuropathological and morphometric investigations.** *Acta Neuropathol (Berl)* 2000;99:365–370
57. Kumada S, Hayashi M, Mizuguchi M, Nakano I, Morimatsu Y, Oda M. **Cerebellar degeneration in hereditary dentatorubral-pallidoluysian atrophy and Machado-Joseph disease.** *Acta Neuropathol (Berl)* 2000;99:48–54
58. Mizusawa H, Yen SH, Hirano A, Llena JF. **Pathology of the dentate nucleus in progressive supranuclear palsy: a histological, immunohistochemical and ultrastructural study.** *Acta Neuropathol (Berl)* 1989;78:419–428
59. Farina L, Nardocci N, Bruzzone MG, et al. **Infantile neuroaxonal dystrophy: neuroradiological studies in 11 patients.** *Neuroradiology* 1999;41:376–380
60. Pena JA, Molina O, Cardozo J. **Hallervorden-Spatz disease: two new early childhood onset cases.** *J Child Neurol* 2000;15:30–32
61. Koeppen AH, Dickson AC, Lamarche JB, Robitaille Y. **Synapses in the hereditary ataxias.** *J Neuropathol Exp Neurol* 1999;58: 748–764
62. Vernino S, Lennon VA. **New Purkinje cell antibody (PCA-2): marker of lung cancer-related neurological autoimmunity.** *Ann Neurol* 2000;47:297–305
63. Hahn A, Claviez A, Brinkmann G, Altermatt HJ, Schneppenheim R, Stephani U. **Paraneoplastic cerebellar degeneration in pediatric Hodgkin disease.** *Neuropediatrics* 2000;31:42–44
64. Antunes NL, Khakoo Y, Matthay KK, et al. **Antineuronal antibodies in patients with neuroblastoma and paraneoplastic opsoclonus-myoclonus.** *J Pediatr Hematol Oncol* 2000;22:315–320
65. Tanji K, Vu TH, Schon EA, DiMauro S, Bonilla E. **Kearns-Sayre syndrome: unusual pattern of expression of subunits of the respiratory chain in the cerebellar system.** *Ann Neurol* 1999;45:377–383
66. Zhou L, Chomyn A, Attardi G, Miller CA. **Myoclonic epilepsy and ragged red fibers (MERRF) syndrome: selective vulnerability of CNS neurons does not correlate with the level of mitochondrial tRNAlys mutation in individual neuronal isolates.** *J Neurosci* 1997; 17:7746–7753
67. Barkhof F, Verrips A, Wesseling P, et al. **Cerebrotendinous xanthomatosis: the spectrum of imaging findings and the correlation with neuropathologic findings.** *Radiology* 2000;217:869–876
68. Breidahl WH, Ives FJ, Khangure MS. **Cerebral and brain stem Langerhans cell histiocytosis.** *Neuroradiology* 1993;35:349–351